

An LLM-enabled Multi-Agent Autonomous Mechatronics Design Framework

Zeyu Wang¹, Frank P.-W. Lo¹, Qian Chen¹, Yongqi Zhang¹, Chen Lin¹, Xu Chen¹, Zhenhua Yu²,
Alexander J. Thompson¹, Eric M. Yeatman^{1*}, Benny P. L. Lo^{1*}

¹Imperial College London, London, UK

²Univeristy of Aberdeen, Aberdeen, UK

e.yeatman@imperial.ac.uk, benny.lo@imperial.ac.uk

Abstract

Existing LLM-enabled multi-agent frameworks are predominantly limited to digital or simulated environments and confined to narrowly focused knowledge domain, constraining their applicability to complex engineering tasks that require the design of physical embodiment, cross-disciplinary integration, and constraint-aware reasoning. This work proposes a multi-agent autonomous mechatronics design framework, integrating expertise across mechanical design, optimization, electronics, and software engineering to autonomously generate functional prototypes with minimal direct human design input. Operating primarily through a language-driven workflow, the framework incorporates structured human feedback to ensure robust performance under real-world constraints. To validate its capabilities, the framework is applied to a real-world challenge involving autonomous water-quality monitoring and sampling, where traditional methods are labor-intensive and ecologically disruptive. Leveraging the proposed system, a fully functional autonomous vessel was developed with optimized propulsion, cost-effective electronics, and advanced control. The design process was carried out by specialized agents, including a high-level planning agent responsible for problem abstraction and dedicated agents for structural, electronics, control, and software development. This approach demonstrates the potential of LLM-based multi-agent systems to automate real-world engineering workflows and reduce reliance on extensive domain expertise.

1. Introduction

In the last few years, large language models (LLMs) [1–3] have made rapid progress across a wide range of cognitive tasks, including natural language understanding [4], code generation [5, 6], symbolic reasoning [7, 8], and scientific problem-solving [9, 10]. Powered by transformer architectures [11, 12] and trained on massive dataset, models such

as GPT-4 [13], Claude [14], DeepSeek [15], and PaLM [16] exhibit strong performance in chain-of-thought reasoning [17, 18], few-shot learning [19, 20], and even multimodal understanding when extended to vision-language settings [21, 22]. These capabilities have enabled LLMs to perform not only linguistic tasks, but also to engage in procedural synthesis [23], and structured decision-making [24, 25], laying the foundation for their integration into agent-based systems capable of autonomous planning and tool use.

The rise of agent-based systems [26] marks a critical milestone in artificial intelligence, enabling entities to autonomously perceive, reason, and act within specific environments [27]. LLM-driven agents [28] further enhance these capabilities through sophisticated linguistic comprehension and generation, proving effective in diverse applications such as text summarization [29], software debugging [30, 31], documentation automation [32, 33], customer support [34, 35], mathematical theorem synthesis [36, 37], virtual environment navigation [38], and structured data querying [39, 40]. In industry, LLM agents have streamlined narrowly defined workflows, including report generation [41–43] and basic data analytics [44, 45], significantly improving operational efficiency.

However, current LLM-based agent implementations remain primarily confined to digital or simulated environments, thus limiting their practical application in complex engineering tasks which require the design of physical embodiment, cross-domain integration, and constraint-aware reasoning. Recent attempts to bridge this gap have emerged, demonstrating initial integration of LLM agents with physical experimentation in domains such as autonomous chemical synthesis [46], materials design [47–49], drug discovery [50], and adaptive multi-agent manufacturing systems [51]. Despite these advancements, little attention has been given to LLM-enabled multi-agent frameworks targeting autonomous mechatronics design, a field inherently requiring multidisciplinary expertise across mechanical engineering, electronics, control systems, and software development. The inherent complexity of mechatronics de-

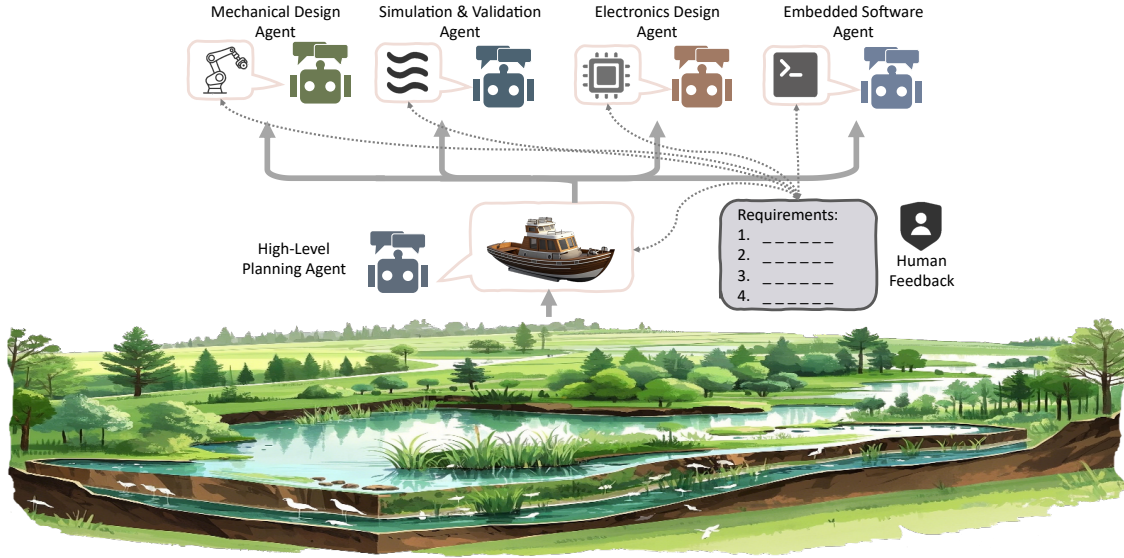


Figure 1. Conceptual architecture of the autonomous mechatronics design framework, illustrating multi-agent collaboration for system development with human-in-the-loop feedback.

sign presents significant barriers to expertise and innovation, yet the cross-domain knowledge synthesis capabilities of LLMs offer emerging potential to support and accelerate certain aspects of mechatronics development. Leveraging LLMs could democratize access to mechatronics design, streamline the development process, and foster innovation by reducing the dependency on domain experts. Addressing this research gap, we propose an LLM-enabled multi-agent framework for autonomous mechatronics system design, specifically targeting complex, interdisciplinary engineering challenges involving real-world physical embodiment. To illustrate the framework effectiveness, we apply it to an autonomous water-quality monitoring applications for wetlands [52, 53]—an ecologically critical yet traditionally labor-intensive and expensive task. Leveraging specialized collaborative agents guided by structured human feedback, our approach significantly reduces complexity and streamline the processes. The resulting autonomous vessel demonstrates practical environmental monitoring potential, validating the proposed method and underscoring the potential of LLM-based agents in reshaping mechatronics design paradigms. This scalable framework could broadly facilitate future advances in areas such as biorobotics for precision medicine [54, 55], autonomous surgical robotics [56, 57], and AI-enabled multimodal health monitoring [58], significantly lowering barriers and expanding participation in interdisciplinary engineering innovation.

2. Intelligence Levels Definition

We proposed Intelligence Levels for Autonomous Mechatronics Design (AMD Levels) as followings:

- **AMD Level 0 – Manual Design:** Entirely human-driven; all tasks and integration are performed manually.
- **AMD Level 1 – Assisted Automation:** Limited AI support (e.g., retrieval, basic code); decision-making remains fully human-controlled.
- **AMD Level 2 – Semi-Autonomous Design:** The system autonomously executes domain-specific tasks; humans manage integration and validation.
- **AMD Level 3 – Highly Autonomous Design:** Cross-domain coordination is automated; human involvement is restricted to high-level supervision and final evaluation.
- **AMD Level 4 – Fully Autonomous Design:** End-to-end automation. The system independently handles planning, integration, optimization, and validation, with human input limited to objectives setting and outcome assessment.

3. Methodology

3.1. Framework design

The proposed employs a hierarchical architecture governed by a High-Level Planning Agent, which decomposes complex challenges into modular tasks for domain-specific agents. Each agent autonomously generates, refines, and validates designs within its specialized discipline, while structured human input ensures feasibility and compliance with practical constraints.

Taking the autonomous water-quality monitoring and sampling system as an example, the High-Level Planning Agent initially analyzes functional requirements—such as mobility, environmental adaptability, and energy efficiency—to define the optimal configuration: a compact,

dual-propeller vessel. Subsequently, the Mechanical Design Agent optimizes the propeller and hull structures, validated by the Simulation & Validation Agent using computational fluid dynamics (CFD) and Finite Elements Analysis (FEA) for hydrodynamics and structural integrity. The Electronics Design Agent synthesizes propulsion and control circuits, leveraging available hardware to simplify integration. The Embedded Software Agent then generates motor-control and communication firmware, for optimal control of the hardware components. Meanwhile, human feedback is introduced as an external input, guiding the agents through ambiguous design choices and refining their outputs where limitations arise. This multi-agent approach integrates high-level objectives with low-level implementation, significantly reduce the iterative design process and dependency on domain experts, providing a scalable methodology for autonomous mechatronics design.

3.2. High-Level Planning Agent

The High-Level Planning Agent translates system-level requirements into actionable design objectives, guiding downstream engineering tasks. Leveraging LLM-based decision-making, it integrates functional goals, constraints, and human feedback into a unified design strategy. Mathematically, the agent’s function can be expressed as:

$$P = f(F, C, H) \quad (1)$$

where F denotes the functional requirements (e.g., mobility, energy efficiency, environmental adaptability), C represents system constraints, and H refers to human feedback. By incorporating human feedback [59] directly into this loop, the agent ensures real-world insights continuously shape the design path, enabling robust, adaptable, and manufacturable mechatronic solutions.

3.3. Mechanical Design Agent

Mechanical design integrates structural mechanics [60], fluid dynamics [61], and manufacturability considerations [62] to ensure functional performance and production feasibility. Traditionally, engineers employ parametric modeling [63], finite element analysis [64], and iterative refinement, balancing constraints, such as material properties, hydrodynamic efficiency [65], and structural integrity. This requires substantial computational expertise, geometric reasoning, and practical fabrication experiences and knowledge. However, current LLMs face intrinsic limitations in mechanical design due to insufficient spatial reasoning and geometric cognition [66]. Unlike natural language processing or code generation, mechanical design inherently relies on real-time spatial visualization and parametric interaction—capabilities central to traditional CAD tools (e.g., SolidWorks [67], Fusion 360 [68], COMSOL [69]) yet largely absent in existing LLMs. Additionally, mechanical

design demands intuitive understanding of manufacturability constraints and material properties, which LLMs struggle to infer from text-based training alone.

To address these challenges, we propose a hybrid approach combining LLM-driven geometry generation and targeted human-in-the-loop feedback. This structured methodology forms the basis of our Mechanical Design Agent, enabling autonomous, and iterative optimization of mechanical structures yielding functional and effective mechanical designs. Specifically, the Mechanical Design Agent autonomously interprets high-level functional requirements to generate and refine mechanical components. For example, in designing the autonomous water-quality monitoring system, the agent iteratively optimizes the propeller and hull structures, systematically improving their stability, hydrodynamic efficiency, and manufacturability. This design workflow involves three structured stages: parametric geometric modeling, airfoil section generation, and transformation of 2D airfoil profiles into finalized 3D blade geometries.

Specifically, an LLM-driven mapping function formalizes this process:

$$\mathcal{L}: \mathcal{P} \rightarrow \mathcal{C} \quad (2)$$

where \mathcal{P} denotes the set of design parameters (e.g., blade root and tip chords, pitch angles, airfoil thickness, rake/skew angles) and \mathcal{C} represents the generated CAD code. Iterative refinement is achieved via:

$$\mathcal{P}_{n+1} = \mathcal{F}(\mathcal{P}_n, R_n) \quad (3)$$

with R_n denoting simulation feedback at iteration n .

a) Parametric Geometric Modeling

The blade is defined along its span $z \in [0, L]$ by introducing the normalized coordinate:

$$r = \frac{z}{L}, \quad r \in [0, 1] \quad (4)$$

Two primary functions govern the blade geometry: Chord Distribution $C(z)$ is defined as:

$$C(z) = C_r + (C_t - C_r)r \quad (5)$$

where C_r and C_t are the chord lengths at the root and tip, respectively. More complex variations (e.g., incorporating a Gaussian bulge) are expressed as:

$$C(z) = [C_r + (C_t - C_r)r] [1 + \beta \exp(-\gamma(r - r_0)^2)] \quad (6)$$

with β , γ , and r_0 as design parameters. Pitch Distribution $\alpha(z)$ is defined as:

$$\alpha(z) = \alpha_r + (\alpha_t - \alpha_r)r \quad (7)$$

where α_r and α_t are the pitch angles (in radians) at the root and tip.

b) Airfoil Generation

The agent generates a 2D airfoil profile at each span-wise station using a parameterized thickness distribution function $f(x)$, defined over the chord-wise coordinate $x \in [0, 1]$. In general, the upper and lower surfaces are given by:

$$\{(x - x_0, +f(x))\} \quad \text{and} \quad \{(x - x_0, -f(x))\} \quad (8)$$

c) Transformation of 2D Airfoil Sections into a 3D Blade

Each generated 2D airfoil section is transformed into its 3D location by applying:

Scaling: The normalized airfoil coordinates (x, y) are scaled by the local chord $C(z)$:

$$X = C(z)x, \quad Y = C(z)S(z)y \quad (9)$$

where $S(z)$ is an optional thickness scaling factor.

Rotation (Twist): The scaled coordinates are rotated by the local pitch angle $\alpha(z)$:

$$X_r = X \cos \alpha(z) - Y \sin \alpha(z) \quad (10)$$

$$Y_r = X \sin \alpha(z) + Y \cos \alpha(z) \quad (11)$$

Translation (Rake and Skew): To capture planform effects, a translation is applied:

$$S_{\text{rake}}(z) = -z \tan(\theta_{\text{rake}}) \quad (12)$$

$$S_{\text{skew}}(z) = rL \tan(\theta_{\text{skew}}) \quad (13)$$

The final coordinates become:

$$X_f = X_r + S_{\text{skew}}(z) \quad (14)$$

$$Y_f = Y_r + S_{\text{rake}}(z) \quad (15)$$

3.4. Simulation & Validation Agent

Structural validation is essential for mechatronic systems, ensuring robustness and reliability under operational conditions. Traditionally, engineers employ FEA and computational methods to assess structural integrity, deformation, and stress distribution, guiding material selection, geometric optimization, and load-bearing capacity. Integrating LLMs into simulation-driven workflows could accelerate the in structural validation tasks such as model configuration and boundary condition definition. However, current LLMs struggle with interpreting complex multiphysics phenomena, non-linear material behaviors, and ensuring numerical convergence, thus necessitating a hybrid approach that combines AI-driven methodologies with empirical validation.

Within the proposed framework, the Simulation & Validation Agent autonomously validates mechanical structures

generated by the Mechanical Design Agent. Specifically, it automatically configures simulations, defines materials and boundary conditions, and performs physics-based analyses using finite element methods. Results from these simulations guide iterative design refinement to enhance structural performance and manufacturability. For validating the autonomous boat's propulsion system, the agent employs CFD and structural FEA, evaluating fluid-structure interactions, mechanical stresses under operational loads, and potential fatigue points.

Initially, to establish baseline safety margins, the agent performed a fully coupled fluid-structure interaction (FSI) simulation under laminar flow conditions as a baseline analysis, offering insights into stress distribution and potential failure regions under extreme passive exposure. Specifically, the agent sets up a FSI interface [70] to transfer pressure and shear to the blades, followed by a stationary stress analysis computing von Mises stress:

$$\sigma_{vM} = \sqrt{0.5 [(\sigma_1 - \sigma_2)^2 + (\sigma_2 - \sigma_3)^2 + (\sigma_3 - \sigma_1)^2]} \quad (16)$$

with σ_1 , σ_2 , and σ_3 being the principal stresses.

Subsequently, to model the propeller's high-speed rotation and fluid interaction, the agent uses rotating machinery analysis in COMSOL, solving the Reynolds-Averaged Navier-Stokes (RANS) equations [71] with the Shear Stress Transport (SST) turbulence model [72]. A rotating reference frame is applied to the propeller domain, with the surrounding fluid kept stationary to ensure proper interface conditions. The momentum equation in the rotating frame is given by:

$$\rho(\mathbf{u} \cdot \nabla \mathbf{u}) = -\nabla p + \nabla \cdot [\mu_{\text{eff}}(\nabla \mathbf{u} + (\nabla \mathbf{u})^T)] + F_{\text{rot}} \quad (17)$$

where ρ is the fluid density, \mathbf{u} is the velocity field, p is the pressure, and $\mu_{\text{eff}} = \mu_t + \mu$ is the effective viscosity accounting for both molecular (μ) and turbulent (μ_t) contributions. The term F_{rot} encompasses Coriolis and centrifugal forces. By blending $k-\omega$ and $k-\epsilon$ formulations [73, 74], the SST model ensures accurate near-wall treatment and robust free-stream predictions.

3.5. Electronics Design Agent

Electrical engineering design involves circuit analysis, electronics design, signal processing, control systems, and embedded computing to develop robust electronic systems. Traditional workflows include schematic design, component selection, PCB layout [75], and system-level testing, which require expertise in electromagnetic compatibility (EMC), thermal management, and manufacturability. Recent advancements in LLMs offer transformative potential by assisting in tasks, such as automated component selection [76], schematic generation, and design optimization. Trained on extensive technical documentation, these models can efficiently parse datasheets, recommend suitable

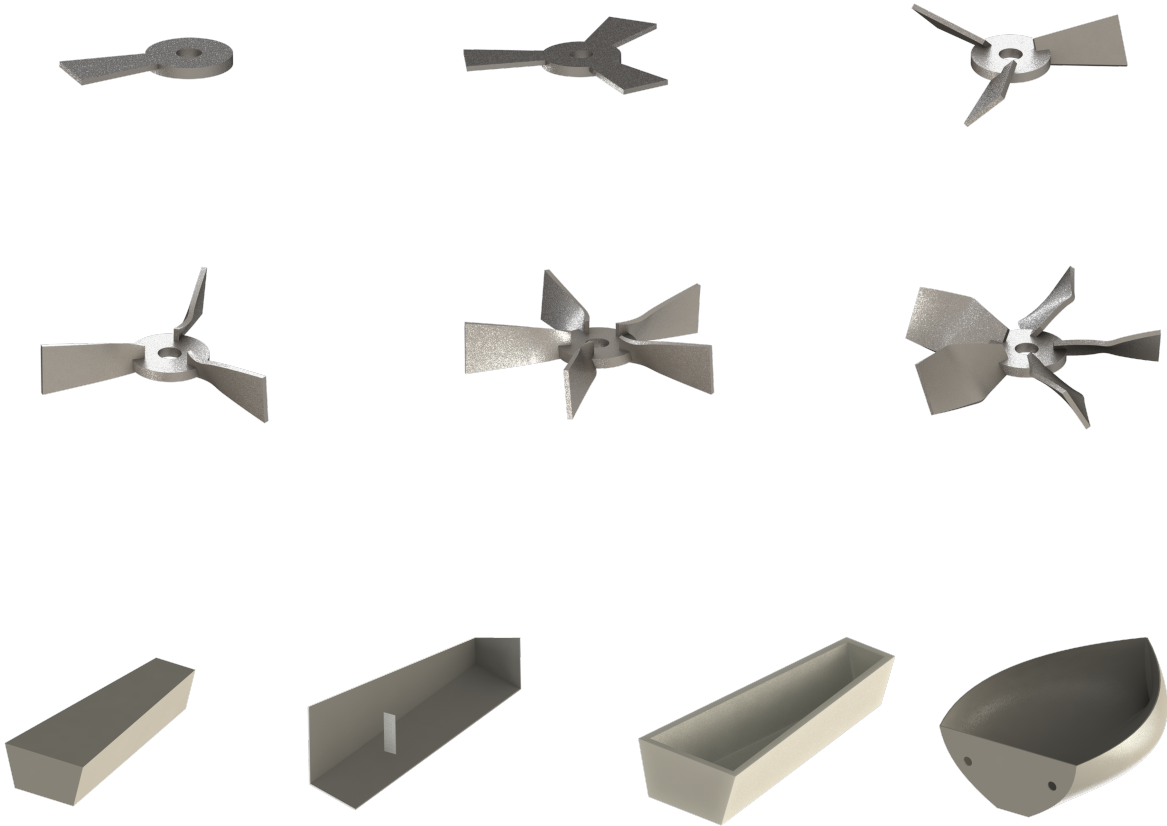


Figure 2. Iterative design process of propellers and hulls generated by the Mechanical Design Agent.

components, and streamline procurement processes, significantly reducing design cycles.

However, LLMs currently face limitations in real-time design constraints, and robustness under practical constraints. To overcome these limitations, the Electronics Design Agent is designed to employ a hybrid workflow that integrates LLM-based reasoning, structured human feedback, and existing hardware utilization. Rather than designing circuits from scratch, the agent first evaluates available hardware resources for potential reuse, optimizing resource efficiency and accelerating development.

3.6. Embedded Software Agent

Embedded systems serve as computational backbones in mechatronics design, translating high-level objectives into precise control commands [77]. Effective embedded software design requires expertise in real-time control algorithms, communication protocols, firmware development, and sensor-driven actuation. Recent advances in LLMs offer opportunities for automating embedded software tasks, including firmware generation, adaptive control logic optimization, and efficient resource allocation. Trained on extensive programming datasets, LLMs can autonomously

generate structured code and adapt existing control strategies. However, current LLM-driven code still faces limitations in real-time execution efficiency and direct peripheral interaction, thus necessitating empirical validation.

Within our framework, the Embedded Software Agent translates high-level specifications into executable firmware tailored specifically to hardware architectures defined by the Electronics Design Agent. This inter-agent coordination ensures seamless integration between hardware and software. Additionally, the agent implements adaptive motor-control strategies essential for tasks such as differential speed control in rudderless propulsion systems, dynamically adjusting motor actuation to achieve reach the targets precisely under varying operational conditions.

4. Experimental Results

4.1. Mechanical Design Agent

Guided by the autonomous boat objective established by the High-Level Planning Agent, the Mechanical Design Agent iteratively optimized the propeller and hull structures, as shown in Fig. 2. The propeller design process, illustrated in the top two rows of Fig. 2, began with a three-bladed

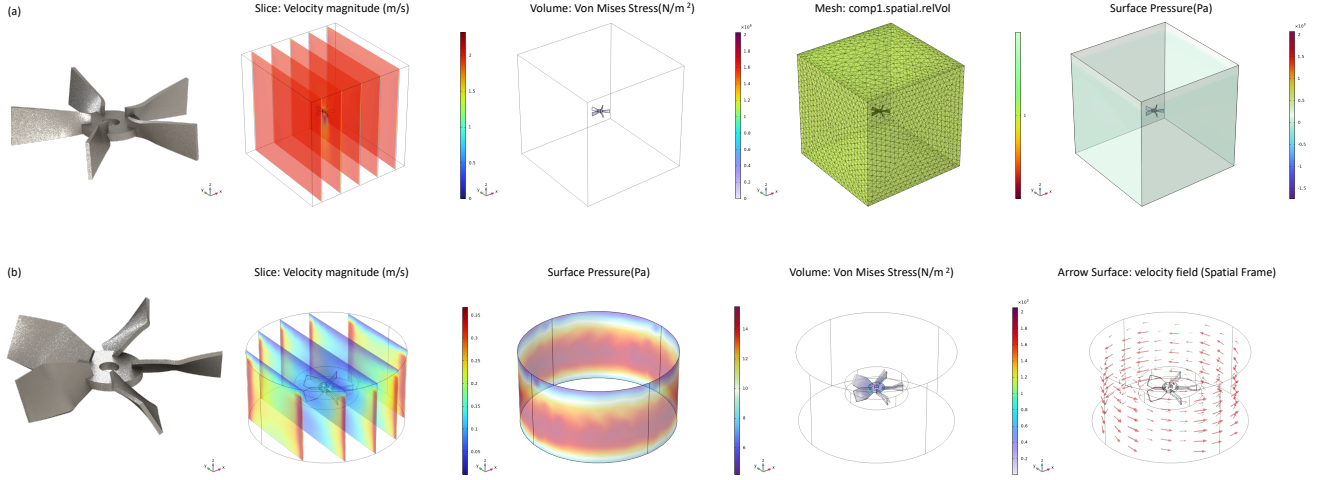


Figure 3. CFD and structural analysis of the optimized propeller design performed by the Simulation & Validation Agent. (a) Structural stress distribution under laminar flow conditions (baseline analysis). (b) Results obtained from rotating turbulent flow analysis using the Shear Stress Transport (SST) model. Results demonstrate stable hydrodynamic performance, reasonable structural stress levels, and highlight areas for further refinement.

configuration featuring a blade length of 26 mm and a hub diameter of 20 mm. Early iterations exhibited poor hydrodynamic performance. Through successive refinements in blade curvature, twist angle, and hub-to-blade ratio, the agent improved hydrodynamic efficiency by enhancing the lift-to-drag ratio and mitigating flow separation. The final geometry balances structural rigidity with stable thrust generation.

Retrieving the detailed implementation of agent, the agent tailored chord and pitch distributions to maximize mid-span loading using piecewise interpolation, as shown below:

$$C(z) = \begin{cases} C_r + (C_m - C_r)(2r), & 0 \leq r \leq 0.5 \\ C_m + (C_t - C_m)(2r + 1), & 0.5 \leq r \leq 1 \end{cases} \quad (18)$$

with C_m as the maximum chord at mid-span. The pitch distribution is similarly interpolated:

$$\alpha(z) = \begin{cases} \alpha_r + (\alpha_m - \alpha_r)(2r), & 0 \leq r \leq 0.5 \\ \alpha_m + (\alpha_t - \alpha_m)(2r + 1), & 0.5 \leq r \leq 1 \end{cases} \quad (19)$$

Generic airfoil sections were generated and transformed into a finalized three-dimensional blade geometry optimized for thrust.

The bottom row of Fig. 2 illustrates the hull design evolution. Initial outputs consisted of solid rectangular forms that failed to satisfy buoyancy and weight constraints. Later iterations introduced hollowed structures, though early designs lacked viable compartmentalization. Through progressive refinement, the agent incorporated internal reinforcements, strategic cutouts, and streamlined contours,

resulting in a curved bow design that reduces drag, improves maneuverability, and accommodates onboard components. These results demonstrate the Mechanical Design Agent's capacity for autonomous structural refinement under evolving constraints, producing mechanically feasible and performance-optimized components suitable for downstream validation

4.2. Simulation & Validation Agent

To evaluate the propeller design generated by the Mechanical Design Agent, the Simulation & Validation Agent conducted a two-stage CFD analysis, as shown in Fig. 3. For the initial baseline analysis, the agent autonomously performed a laminar-flow fluid-structure interaction simulation using, as an example, the fifth design iteration shown in Fig. 2. The resulting velocity magnitude slices and surface pressure distributions confirmed smooth flow behavior, minimal separation, and coherent pressure fields, validating early-stage design stability. Given the high Reynolds number regime of the final propeller configuration, the agent transitioned to a turbulence-resolving analysis, employing the SST model for enhanced fidelity in near-wall flow characterization, again exemplified by the final iteration shown in Fig. 2. Unlike the baseline scenario, however, the agent could not autonomously configure this turbulent-flow analysis, requiring substantial human feedback and expert assistance to iteratively adjust solver settings, boundary conditions, and spatial discretization until convergence. Further detailed validation of these results remains necessary to fully ensure accuracy and reliability.

Despite demonstrating physics module inference, the Simulation & Validation Agent remains limited in execu-

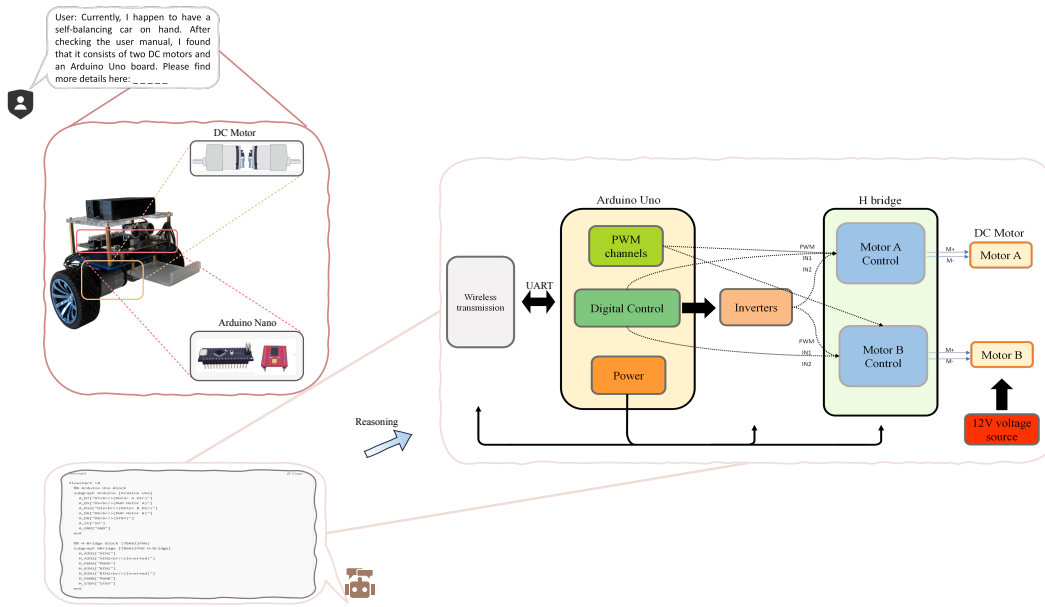


Figure 4. Electronics Design Agent workflow based on user feedback. The agent analyzes the existing balance car system and reconstructs the core control architecture, including Arduino-based PWM control and H-bridge motor driving

tion. Configuration inconsistencies—partly due to software interface variability—undermine its reliability across solver settings. Defining boundary conditions and spatial domain partitioning remains particularly challenging, constrained by the agent’s lack of geometric intuition and visuospatial inference capability. These limitations are pronounced in transient, multiphysics simulations, where complex temporal and inter-domain dependencies often lead to convergence failure. Addressing these challenges will require integration of structured expert priors, few-shot learning from validated workflows, and physics-informed guidance to systematically elevate robustness and generalizability.

4.3. Electronics Design Agent

To evaluate the agent’s adaptive design capability, an Arduino Nano-based self-balancing car was introduced as external input. The agent received specifications of the system, including motor drivers and power modules, and assessed whether its components could be disassembled and reconfigured into a functional propulsion system for the autonomous boat.

As shown in Fig. 4, the Electronics Design Agent synthesized a system architecture that repurposes the self-balancing car hardware for dual-motor actuation. Leveraging circuit knowledge and structured human input, the agent analyzed the feasibility of reusing the motor control, power distribution, and signal processing elements to construct an efficient and compact drive system.

The resulting architecture comprises two subsystems: the Arduino Nano control unit and an H-bridge motor

driver. Pulse-width modulation (PWM) signals from the control unit are processed via logic circuitry and inverters to regulate motor speed and direction. The H-bridge enables bidirectional current flow for two independently controlled DC motors, each powered by a 12V source. Differential motor speed control provides rudderless steering, enabling smooth turning and precise navigation—crucial for autonomous vessels operations. Wireless transmission further supports remote operation in real-world environments.

4.4. Embedded Software Agent

Fig. 5 presents the embedded firmware architecture structured by the agent. The system initializes by configuring GPIOs and peripherals, then continuously monitors incoming serial data. Upon receiving a complete command, it parses the motion type—such as forward, backward, left, right, or stop—and generates corresponding PWM signals to control Motor A and Motor B via an H-bridge driver. For turning maneuvers, the agent applies differential velocity control, adjusting motor speeds to modulate turning radius without the need for a physical rudder.

Real-world execution is assessed using logic analyzer traces, as shown in Fig. 5, which capture IN1, IN2, and PWM signals for both motors under various commands. The observed duty cycles—39.2% (forward), 31.4% (backward), 58.8% (left), and 15.7% (right)—confirm precise motor actuation aligned with the embedded control logic. Directional transitions are accurately executed through appropriate phase shifting. A minor deviation was observed in the first PWM pulse during turning, attributed to initializa-

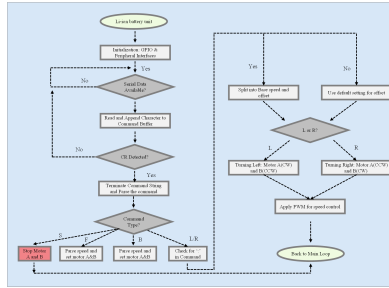
User: Could you help me write a piece of code based on the electrical engineer's comments?

```

% Parameters
% Motor
% Motor 1
% Motor 2
% Motor 3
% Motor 4
% Motor 5
% Motor 6
% Motor 7
% Motor 8
% Motor 9
% Motor 10
% Motor 11
% Motor 12
% Motor 13
% Motor 14
% Motor 15
% Motor 16
% Motor 17
% Motor 18
% Motor 19
% Motor 20
% Motor 21
% Motor 22
% Motor 23
% Motor 24
% Motor 25
% Motor 26
% Motor 27
% Motor 28
% Motor 29
% Motor 30
% Motor 31
% Motor 32
% Motor 33
% Motor 34
% Motor 35
% Motor 36
% Motor 37
% Motor 38
% Motor 39
% Motor 40
% Motor 41
% Motor 42
% Motor 43
% Motor 44
% Motor 45
% Motor 46
% Motor 47
% Motor 48
% Motor 49
% Motor 50
% Motor 51
% Motor 52
% Motor 53
% Motor 54
% Motor 55
% Motor 56
% Motor 57
% Motor 58
% Motor 59
% Motor 60
% Motor 61
% Motor 62
% Motor 63
% Motor 64
% Motor 65
% Motor 66
% Motor 67
% Motor 68
% Motor 69
% Motor 70
% Motor 71
% Motor 72
% Motor 73
% Motor 74
% Motor 75
% Motor 76
% Motor 77
% Motor 78
% Motor 79
% Motor 80
% Motor 81
% Motor 82
% Motor 83
% Motor 84
% Motor 85
% Motor 86
% Motor 87
% Motor 88
% Motor 89
% Motor 90
% Motor 91
% Motor 92
% Motor 93
% Motor 94
% Motor 95
% Motor 96
% Motor 97
% Motor 98
% Motor 99
% Motor 100
% Motor 101
% Motor 102
% Motor 103
% Motor 104
% Motor 105
% Motor 106
% Motor 107
% Motor 108
% Motor 109
% Motor 110
% Motor 111
% Motor 112
% Motor 113
% Motor 114
% Motor 115
% Motor 116
% Motor 117
% Motor 118
% Motor 119
% Motor 120
% Motor 121
% Motor 122
% Motor 123
% Motor 124
% Motor 125
% Motor 126
% Motor 127
% Motor 128
% Motor 129
% Motor 130
% Motor 131
% Motor 132
% Motor 133
% Motor 134
% Motor 135
% Motor 136
% Motor 137
% Motor 138
% Motor 139
% Motor 140
% Motor 141
% Motor 142
% Motor 143
% Motor 144
% Motor 145
% Motor 146
% Motor 147
% Motor 148
% Motor 149
% Motor 150
% Motor 151
% Motor 152
% Motor 153
% Motor 154
% Motor 155
% Motor 156
% Motor 157
% Motor 158
% Motor 159
% Motor 160
% Motor 161
% Motor 162
% Motor 163
% Motor 164
% Motor 165
% Motor 166
% Motor 167
% Motor 168
% Motor 169
% Motor 170
% Motor 171
% Motor 172
% Motor 173
% Motor 174
% Motor 175
% Motor 176
% Motor 177
% Motor 178
% Motor 179
% Motor 180
% Motor 181
% Motor 182
% Motor 183
% Motor 184
% Motor 185
% Motor 186
% Motor 187
% Motor 188
% Motor 189
% Motor 190
% Motor 191
% Motor 192
% Motor 193
% Motor 194
% Motor 195
% Motor 196
% Motor 197
% Motor 198
% Motor 199
% Motor 200
% Motor 201
% Motor 202
% Motor 203
% Motor 204
% Motor 205
% Motor 206
% Motor 207
% Motor 208
% Motor 209
% Motor 210
% Motor 211
% Motor 212
% Motor 213
% Motor 214
% Motor 215
% Motor 216
% Motor 217
% Motor 218
% Motor 219
% Motor 220
% Motor 221
% Motor 222
% Motor 223
% Motor 224
% Motor 225
% Motor 226
% Motor 227
% Motor 228
% Motor 229
% Motor 230
% Motor 231
% Motor 232
% Motor 233
% Motor 234
% Motor 235
% Motor 236
% Motor 237
% Motor 238
% Motor 239
% Motor 240
% Motor 241
% Motor 242
% Motor 243
% Motor 244
% Motor 245
% Motor 246
% Motor 247
% Motor 248
% Motor 249
% Motor 250
% Motor 251
% Motor 252
% Motor 253
% Motor 254
% Motor 255
% Motor 256
% Motor 257
% Motor 258
% Motor 259
% Motor 260
% Motor 261
% Motor 262
% Motor 263
% Motor 264
% Motor 265
% Motor 266
% Motor 267
% Motor 268
% Motor 269
% Motor 270
% Motor 271
% Motor 272
% Motor 273
% Motor 274
% Motor 275
% Motor 276
% Motor 277
% Motor 278
% Motor 279
% Motor 280
% Motor 281
% Motor 282
% Motor 283
% Motor 284
% Motor 285
% Motor 286
% Motor 287
% Motor 288
% Motor 289
% Motor 290
% Motor 291
% Motor 292
% Motor 293
% Motor 294
% Motor 295
% Motor 296
% Motor 297
% Motor 298
% Motor 299
% Motor 300
% Motor 301
% Motor 302
% Motor 303
% Motor 304
% Motor 305
% Motor 306
% Motor 307
% Motor 308
% Motor 309
% Motor 310
% Motor 311
% Motor 312
% Motor 313
% Motor 314
% Motor 315
% Motor 316
% Motor 317
% Motor 318
% Motor 319
% Motor 320
% Motor 321
% Motor 322
% Motor 323
% Motor 324
% Motor 325
% Motor 326
% Motor 327
% Motor 328
% Motor 329
% Motor 330
% Motor 331
% Motor 332
% Motor 333
% Motor 334
% Motor 335
% Motor 336
% Motor 337
% Motor 338
% Motor 339
% Motor 340
% Motor 341
% Motor 342
% Motor 343
% Motor 344
% Motor 345
% Motor 346
% Motor 347
% Motor 348
% Motor 349
% Motor 350
% Motor 351
% Motor 352
% Motor 353
% Motor 354
% Motor 355
% Motor 356
% Motor 357
% Motor 358
% Motor 359
% Motor 360
% Motor 361
% Motor 362
% Motor 363
% Motor 364
% Motor 365
% Motor 366
% Motor 367
% Motor 368
% Motor 369
% Motor 370
% Motor 371
% Motor 372
% Motor 373
% Motor 374
% Motor 375
% Motor 376
% Motor 377
% Motor 378
% Motor 379
% Motor 380
% Motor 381
% Motor 382
% Motor 383
% Motor 384
% Motor 385
% Motor 386
% Motor 387
% Motor 388
% Motor 389
% Motor 390
% Motor 391
% Motor 392
% Motor 393
% Motor 394
% Motor 395
% Motor 396
% Motor 397
% Motor 398
% Motor 399
% Motor 400
% Motor 401
% Motor 402
% Motor 403
% Motor 404
% Motor 405
% Motor 406
% Motor 407
% Motor 408
% Motor 409
% Motor 410
% Motor 411
% Motor 412
% Motor 413
% Motor 414
% Motor 415
% Motor 416
% Motor 417
% Motor 418
% Motor 419
% Motor 420
% Motor 421
% Motor 422
% Motor 423
% Motor 424
% Motor 425
% Motor 426
% Motor 427
% Motor 428
% Motor 429
% Motor 430
% Motor 431
% Motor 432
% Motor 433
% Motor 434
% Motor 435
% Motor 436
% Motor 437
% Motor 438
% Motor 439
% Motor 440
% Motor 441
% Motor 442
% Motor 443
% Motor 444
% Motor 445
% Motor 446
% Motor 447
% Motor 448
% Motor 449
% Motor 450
% Motor 451
% Motor 452
% Motor 453
% Motor 454
% Motor 455
% Motor 456
% Motor 457
% Motor 458
% Motor 459
% Motor 460
% Motor 461
% Motor 462
% Motor 463
% Motor 464
% Motor 465
% Motor 466
% Motor 467
% Motor 468
% Motor 469
% Motor 470
% Motor 471
% Motor 472
% Motor 473
% Motor 474
% Motor 475
% Motor 476
% Motor 477
% Motor 478
% Motor 479
% Motor 480
% Motor 481
% Motor 482
% Motor 483
% Motor 484
% Motor 485
% Motor 486
% Motor 487
% Motor 488
% Motor 489
% Motor 490
% Motor 491
% Motor 492
% Motor 493
% Motor 494
% Motor 495
% Motor 496
% Motor 497
% Motor 498
% Motor 499
% Motor 500
% Motor 501
% Motor 502
% Motor 503
% Motor 504
% Motor 505
% Motor 506
% Motor 507
% Motor 508
% Motor 509
% Motor 510
% Motor 511
% Motor 512
% Motor 513
% Motor 514
% Motor 515
% Motor 516
% Motor 517
% Motor 518
% Motor 519
% Motor 520
% Motor 521
% Motor 522
% Motor 523
% Motor 524
% Motor 525
% Motor 526
% Motor 527
% Motor 528
% Motor 529
% Motor 530
% Motor 531
% Motor 532
% Motor 533
% Motor 534
% Motor 535
% Motor 536
% Motor 537
% Motor 538
% Motor 539
% Motor 540
% Motor 541
% Motor 542
% Motor 543
% Motor 544
% Motor 545
% Motor 546
% Motor 547
% Motor 548
% Motor 549
% Motor 550
% Motor 551
% Motor 552
% Motor 553
% Motor 554
% Motor 555
% Motor 556
% Motor 557
% Motor 558
% Motor 559
% Motor 560
% Motor 561
% Motor 562
% Motor 563
% Motor 564
% Motor 565
% Motor 566
% Motor 567
% Motor 568
% Motor 569
% Motor 570
% Motor 571
% Motor 572
% Motor 573
% Motor 574
% Motor 575
% Motor 576
% Motor 577
% Motor 578
% Motor 579
% Motor 580
% Motor 581
% Motor 582
% Motor 583
% Motor 584
% Motor 585
% Motor 586
% Motor 587
% Motor 588
% Motor 589
% Motor 590
% Motor 591
% Motor 592
% Motor 593
% Motor 594
% Motor 595
% Motor 596
% Motor 597
% Motor 598
% Motor 599
% Motor 600
% Motor 601
% Motor 602
% Motor 603
% Motor 604
% Motor 605
% Motor 606
% Motor 607
% Motor 608
% Motor 609
% Motor 610
% Motor 611
% Motor 612
% Motor 613
% Motor 614
% Motor 615
% Motor 616
% Motor 617
% Motor 618
% Motor 619
% Motor 620
% Motor 621
% Motor 622
% Motor 623
% Motor 624
% Motor 625
% Motor 626
% Motor 627
% Motor 628
% Motor 629
% Motor 630
% Motor 631
% Motor 632
% Motor 633
% Motor 634
% Motor 635
% Motor 636
% Motor 637
% Motor 638
% Motor 639
% Motor 640
% Motor 641
% Motor 642
% Motor 643
% Motor 644
% Motor 645
% Motor 646
% Motor 647
% Motor 648
% Motor 649
% Motor 650
% Motor 651
% Motor 652
% Motor 653
% Motor 654
% Motor 655
% Motor 656
% Motor 657
% Motor 658
% Motor 659
% Motor 660
% Motor 661
% Motor 662
% Motor 663
% Motor 664
% Motor 665
% Motor 666
% Motor 667
% Motor 668
% Motor 669
% Motor 670
% Motor 671
% Motor 672
% Motor 673
% Motor 674
% Motor 675
% Motor 676
% Motor 677
% Motor 678
% Motor 679
% Motor 680
% Motor 681
% Motor 682
% Motor 683
% Motor 684
% Motor 685
% Motor 686
% Motor 687
% Motor 688
% Motor 689
% Motor 690
% Motor 691
% Motor 692
% Motor 693
% Motor 694
% Motor 695
% Motor 696
% Motor 697
% Motor 698
% Motor 699
% Motor 700
% Motor 701
% Motor 702
% Motor 703
% Motor 704
% Motor 705
% Motor 706
% Motor 707
% Motor 708
% Motor 709
% Motor 710
% Motor 711
% Motor 712
% Motor 713
% Motor 714
% Motor 715
% Motor 716
% Motor 717
% Motor 718
% Motor 719
% Motor 720
% Motor 721
% Motor 722
% Motor 723
% Motor 724
% Motor 725
% Motor 726
% Motor 727
% Motor 728
% Motor 729
% Motor 730
% Motor 731
% Motor 732
% Motor 733
% Motor 734
% Motor 735
% Motor 736
% Motor 737
% Motor 738
% Motor 739
% Motor 740
% Motor 741
% Motor 742
% Motor 743
% Motor 744
% Motor 745
% Motor 746
% Motor 747
% Motor 748
% Motor 749
% Motor 750
% Motor 751
% Motor 752
% Motor 753
% Motor 754
% Motor 755
% Motor 756
% Motor 757
% Motor 758
% Motor 759
% Motor 760
% Motor 761
% Motor 762
% Motor 763
% Motor 764
% Motor 765
% Motor 766
% Motor 767
% Motor 768
% Motor 769
% Motor 770
% Motor 771
% Motor 772
% Motor 773
% Motor 774
% Motor 775
% Motor 776
% Motor 777
% Motor 778
% Motor 779
% Motor 780
% Motor 781
% Motor 782
% Motor 783
% Motor 784
% Motor 785
% Motor 786
% Motor 787
% Motor 788
% Motor 789
% Motor 790
% Motor 791
% Motor 792
% Motor 793
% Motor 794
% Motor 795
% Motor 796
% Motor 797
% Motor 798
% Motor 799
% Motor 800
% Motor 801
% Motor 802
% Motor 803
% Motor 804
% Motor 805
% Motor 806
% Motor 807
% Motor 808
% Motor 809
% Motor 810
% Motor 811
% Motor 812
% Motor 813
% Motor 814
% Motor 815
% Motor 816
% Motor 817
% Motor 818
% Motor 819
% Motor 820
% Motor 821
% Motor 822
% Motor 823
% Motor 824
% Motor 825
% Motor 826
% Motor 827
% Motor 828
% Motor 829
% Motor 830
% Motor 831
% Motor 832
% Motor 833
% Motor 834
% Motor 835
% Motor 836
% Motor 837
% Motor 838
% Motor 839
% Motor 840
% Motor 841
% Motor 842
% Motor 843
% Motor 844
% Motor 845
% Motor 846
% Motor 847
% Motor 848
% Motor 849
% Motor 850
% Motor 851
% Motor 852
% Motor 853
% Motor 854
% Motor 855
% Motor 856
% Motor 857
% Motor 858
% Motor 859
% Motor 860
% Motor 861
% Motor 862
% Motor 863
% Motor 864
% Motor 865
% Motor 866
% Motor 867
% Motor 868
% Motor 869
% Motor 870
% Motor 871
% Motor 872
% Motor 873
% Motor 874
% Motor 875
% Motor 876
% Motor 877
% Motor 878
% Motor 879
% Motor 880
% Motor 881
% Motor 882
% Motor 883
% Motor 884
% Motor 885
% Motor 886
% Motor 887
% Motor 888
% Motor 889
% Motor 890
% Motor 891
% Motor 892
% Motor 893
% Motor 894
% Motor 895
% Motor 896
% Motor 897
% Motor 898
% Motor 899
% Motor 900
% Motor 901
% Motor 902
% Motor 903
% Motor 904
% Motor 905
% Motor 906
% Motor 907
% Motor 908
% Motor 909
% Motor 910
% Motor 911
% Motor 912
% Motor 913
% Motor 914
% Motor 915
% Motor 916
% Motor 917
% Motor 918
% Motor 919
% Motor 920
% Motor 921
% Motor 922
% Motor 923
% Motor 924
% Motor 925
% Motor 926
% Motor 927
% Motor 928
% Motor 929
% Motor 930
% Motor 931
% Motor 932
% Motor 933
% Motor 934
% Motor 935
% Motor 936
% Motor 937
% Motor 938
% Motor 939
% Motor 940
% Motor 941
% Motor 942
% Motor 943
% Motor 944
% Motor 945
% Motor 946
% Motor 947
% Motor 948
% Motor 949
% Motor 950
% Motor 951
% Motor 952
% Motor 953
% Motor 954
% Motor 955
% Motor 956
% Motor 957
% Motor 958
% Motor 959
% Motor 960
% Motor 961
% Motor 962
% Motor 963
% Motor 964
% Motor 965
% Motor 966
% Motor 967
% Motor 968
% Motor 969
% Motor 970
% Motor 971
% Motor 972
% Motor 973
% Motor 974
% Motor 975
% Motor 976
% Motor 977
% Motor 978
% Motor 979
% Motor 980
% Motor 981
% Motor 982
% Motor 983
% Motor 984
% Motor 985
% Motor 986
% Motor 987
% Motor 988
% Motor 989
% Motor 990
% Motor 991
% Motor 992
% Motor 993
% Motor 994
% Motor 995
% Motor 996
% Motor 997
% Motor 998
% Motor 999
% Motor 1000

```

Workflow of the embedded algorithm



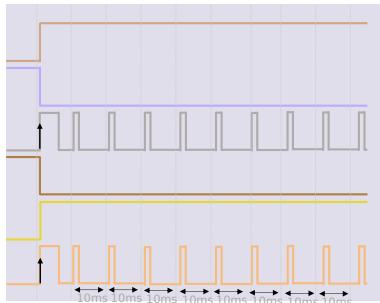
F100
Duty: 39.46% Freq:976.229Hz



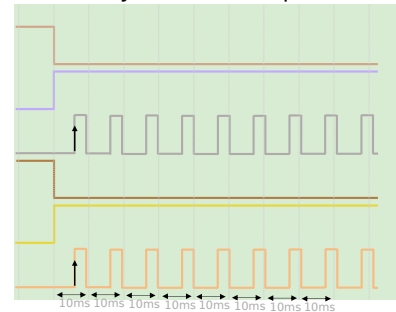
L150
Duty: 58.99% Freq:976.205Hz



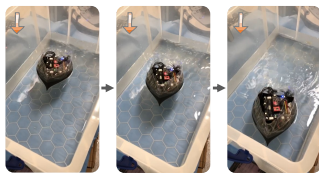
R40
Duty: 16.02% Freq:976.181Hz



B80
Duty: 31.65% Freq:976.205Hz



Forward



Counterclockwise(CCW) Rotation



Clockwise(CW) Rotation

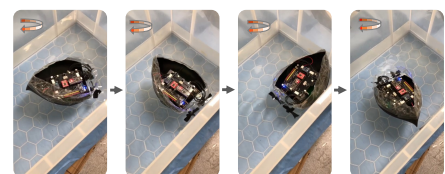


Figure 5. Embedded control logic and human-verified signal outputs. The agent generates control logic based on the Electronics Design Agent’s architecture, while a logic analyzer is used to capture and verify PWM signals under different scenarios.

tion latency from transient register updates. This effect is brief and would not affect the system-level control performance, affirming the agent’s ability to autonomously generate robust, real-time motor control code suitable for autonomous navigation.

5. Discussion

The proposed framework is designed to assist the design of functioning and effective mechatronic systems with structured human feedback. Human guidance proved crucial, particularly for defining modeling sequences in mechanical design tasks. Embedded Software agents demonstrated higher autonomy given clear architectural specifications provided by the Electronics agents, while simple simulations can be autonomously executed via the COMSOL–MATLAB interface, more complex setups—especially involving domain definition and intricate

boundary conditions in multiphysics modules such as transient fluid simulations—remain highly challenging, suggesting the potential benefits of few-shot learning and structured prior injection. Future work will address hardware optimization, such as waterproofing electronic components, and leverage multimodal LLM capabilities, particularly vision-based functionalities, to enhance autonomous control logic.

6. Conclusion

This work introduces an LLM-enabled multi-agent framework that advances autonomous mechatronics design across disciplines boundaries. By integrating language-driven intelligence with structured human feedback, it redefines engineering workflows, lowers expertise barriers, and signals a broader shift toward scalable, democratized innovation in physical-system design.

References

- [1] Yupeng Chang, Xu Wang, Jindong Wang, Yuan Wu, Linyi Yang, Kaijie Zhu, Hao Chen, Xiaoyuan Yi, Cunxiang Wang, Yidong Wang, et al. A survey on evaluation of large language models. *ACM transactions on intelligent systems and technology*, 15(3):1–45, 2024. [1](#)
- [2] Wayne Xin Zhao, Kun Zhou, Junyi Li, Tianyi Tang, Xiaolei Wang, Yupeng Hou, Yingqian Min, Beichen Zhang, Junjie Zhang, Zican Dong, et al. A survey of large language models. *arXiv preprint arXiv:2303.18223*, 1(2), 2023.
- [3] Dorottya Demszky, Diyi Yang, David S Yeager, Christopher J Bryan, Margaret Clapper, Susannah Chandhok, Johannes C Eichstaedt, Cameron Hecht, Jeremy Jamieson, Meghann Johnson, et al. Using large language models in psychology. *Nature Reviews Psychology*, 2(11):688–701, 2023. [1](#)
- [4] Bonan Min, Hayley Ross, Elior Sulem, Amir Poursan Ben Veyseh, Thien Huu Nguyen, Oscar Sainz, Eneko Agirre, Ilana Heintz, and Dan Roth. Recent advances in natural language processing via large pre-trained language models: A survey. *ACM Computing Surveys*, 56(2):1–40, 2023. [1](#)
- [5] Jiawei Liu, Chunqiu Steven Xia, Yuyao Wang, and Lingming Zhang. Is Your Code Generated by ChatGPT Really Correct? Rigorous Evaluation of Large Language Models for Code Generation. *Advances in Neural Information Processing Systems*, 36:21558–21572, December 2023. [1](#)
- [6] Using an LLM to Help With Code Understanding | Proceedings of the IEEE/ACM 46th International Conference on Software Engineering. <https://dl.acm.org/doi/10.1145/3597503.3639187>. [1](#)
- [7] Iman Mirzadeh, Keivan Alizadeh, Hooman Shahrokhi, Oncel Tuzel, Samy Bengio, and Mehrdad Farajtabar. GSM-Symbolic: Understanding the Limitations of Mathematical Reasoning in Large Language Models, October 2024. [1](#)
- [8] Liangming Pan, Alon Albalak, Xinyi Wang, and William Yang Wang. Logic-LM: Empowering Large Language Models with Symbolic Solvers for Faithful Logical Reasoning, October 2023. [1](#)
- [9] Xiaoxuan Wang, Ziniu Hu, Pan Lu, Yanqiao Zhu, Jieyu Zhang, Satyen Subramaniam, Arjun R. Loomba, Shichang Zhang, Yizhou Sun, and Wei Wang. SciBench: Evaluating College-Level Scientific Problem-Solving Abilities of Large Language Models, June 2024. [1](#)
- [10] Qiang et al. Zhang. Scientific Large Language Models: A Survey on Biological & Chemical Domains. *ACM Comput. Surv.*, 57(6):161:1–161:38, February 2025. ISSN 0360-0300. doi: 10.1145/3715318. [1](#)
- [11] Salman Khan, Muzammal Naseer, Munawar Hayat, Syed Waqas Zamir, Fahad Shahbaz Khan, and Mubarak Shah. Transformers in Vision: A Survey. *ACM Comput. Surv.*, 54(10s):200:1–200:41, September 2022. ISSN 0360-0300. doi: 10.1145/3505244. [1](#)
- [12] Ashish Vaswani, Noam Shazeer, Niki Parmar, Jakob Uszkoreit, Llion Jones, Aidan N Gomez, Łukasz Kaiser, and Illia Polosukhin. Attention is All you Need. In *Advances in Neural Information Processing Systems*, volume 30. Curran Associates, Inc., 2017. [1](#)
- [13] OpenAI et al. GPT-4 Technical Report, March 2024. [1](#)
- [14] Aman Priyanshu, Yash Maurya, and Zuofei Hong. AI Governance and Accountability: An Analysis of Anthropic’s Claude, May 2024. [1](#)
- [15] DeepSeek-AI et al. DeepSeek-V3 Technical Report, February 2025. [1](#)
- [16] Rohan et al. Anil. PaLM 2 Technical Report, September 2023. [1](#)
- [17] Jason Wei, Xuezhi Wang, Dale Schuurmans, Maarten Bosma, Brian Ichter, Fei Xia, Ed Chi, Quoc V. Le, and Denny Zhou. Chain-of-Thought Prompting Elicits Reasoning in Large Language Models. *Advances in Neural Information Processing Systems*, 35:24824–24837, December 2022. [1](#)
- [18] Xuan Zhang, Chao Du, Tianyu Pang, Qian Liu, Wei Gao, and Min Lin. Chain of Preference Optimization: Improving Chain-of-Thought Reasoning in LLMs. *Advances in Neural Information Processing Systems*, 37:333–356, December 2024. [1](#)
- [19] Jean-Baptiste Alayrac, Jeff Donahue, Pauline Luc, Antoine Miech, Iain Barr, Yana Hasson, Karel Lenc, Arthur Mensch, Katherine Millican, Malcolm Reynolds, et al. Flamingo: a visual language model for few-shot learning. *Advances in neural information processing systems*, 35:23716–23736, 2022. [1](#)
- [20] Tom Brown, Benjamin Mann, Nick Ryder, Melanie Subbiah, Jared D Kaplan, Prafulla Dhariwal, Arvind Neelakantan, Pranav Shyam, Girish Sastry, Amanda Askell, et al. Language models are few-shot learners. volume 33, pages 1877–1901, 2020. [1](#)
- [21] Deyao Zhu, Jun Chen, Xiaoqian Shen, Xiang Li, and Mohamed Elhoseiny. MiniGPT-4: Enhancing Vision-Language Understanding with Advanced Large Language Models, October 2023. [1](#)
- [22] Jing Yu Koh, Daniel Fried, and Russ R. Salakhutdinov. Generating Images with Multimodal Language Models. *Advances in Neural Information Processing Systems*, 36: 21487–21506, December 2023. [1](#)
- [23] Yixuan Li, Julian Parsert, and Elizabeth Polgreen. Guiding Enumerative Program Synthesis with Large Language Models. In Arie Gurfinkel and Vijay Ganesh, editors, *Computer Aided Verification*, pages 280–301, Cham, 2024. Springer Nature Switzerland. ISBN 978-3-031-65630-9. doi: 10.1007/978-3-031-65630-9_15. [1](#)
- [24] Shuang Li, Xavier Puig, Chris Paxton, Yilun Du, Clinton Wang, Linxi Fan, Tao Chen, De-An Huang, Ekin Akyürek, Anima Anandkumar, Jacob Andreas, Igor Mordatch, Antonio Torralba, and Yuke Zhu. Pre-Trained Language Models for Interactive Decision-Making. *Advances in Neural Information Processing Systems*, 35:31199–31212, December 2022. [1](#)
- [25] Paul Hager, Friederike Jungmann, Robbie Holland, Kunal Bhagat, Inga Hubrecht, Manuel Knauer, Jakob Vielhauer, Marcus Makowski, Rickmer Braren, Georgios Kaissis, and Daniel Rueckert. Evaluation and mitigation of the limitations of large language models in clinical decision-making. *Nature Medicine*, 30(9):2613–2622, September 2024. ISSN 1546-170X. doi: 10.1038/s41591-024-03097-1. [1](#)

- [26] Mark d’Inverno, Michael M Luck, M D’Inverno, and M Luck. *Understanding Agent Systems*. Springer, 2004. 1
- [27] Randall D. Beer. A dynamical systems perspective on agent-environment interaction. *Artificial Intelligence*, 72(1):173–215, January 1995. ISSN 0004-3702. doi: 10.1016/0004-3702(94)00005-L. 1
- [28] Jianing Qiu, Kyle Lam, Guohao Li, Amish Acharya, Tien Yin Wong, Ara Darzi, Wu Yuan, and Eric J Topol. Llm-based agentic systems in medicine and healthcare. *Nature Machine Intelligence*, 6(12):1418–1420, 2024. 1
- [29] Dave Van Veen, Cara Van Uden, Louis Blankemeier, Jean-Benoit Delbrouck, Asad Aali, Christian Bluethgen, Anuj Pareek, Malgorzata Polacin, Eduardo Pontes Reis, Anna Seehofnerová, et al. Adapted large language models can outperform medical experts in clinical text summarization. *Nature medicine*, 30(4):1134–1142, 2024. 1
- [30] Runchu Tian, Yining Ye, Yujia Qin, Xin Cong, Yankai Lin, Yinxu Pan, Yesai Wu, Haotian Hui, Weichuan Liu, Zhiyuan Liu, and Maosong Sun. DebugBench: Evaluating Debugging Capability of Large Language Models, June 2024. 1
- [31] Weiqing Yang, Hanbin Wang, Zhenghao Liu, Xinze Li, Yukun Yan, Shuo Wang, Yu Gu, Minghe Yu, Zhiyuan Liu, and Ge Yu. COAST: Enhancing the Code Debugging Ability of LLMs through Communicative Agent Based Data Synthesis, February 2025. 1
- [32] Jiabo Ye, Anwen Hu, Haiyang Xu, Qinghao Ye, Ming Yan, Yuhao Dan, Chenlin Zhao, Guohai Xu, Chenliang Li, Junfeng Tian, Qian Qi, Ji Zhang, and Fei Huang. mPLUG-DocOwl: Modularized Multimodal Large Language Model for Document Understanding, July 2023. 1
- [33] Yusen Zhang, Ruoxi Sun, Yanfei Chen, Tomas Pfister, Rui Zhang, and Sercan Ö Arık. Chain of Agents: Large Language Models Collaborating on Long-Context Tasks. *Advances in Neural Information Processing Systems*, 37:132208–132237, December 2024. 1
- [34] Shubhra Kanti Karmaker Santu, Parikshit Sondhi, and ChengXiang Zhai. Generative Feature Language Models for Mining Implicit Features from Customer Reviews. In *Proceedings of the 25th ACM International on Conference on Information and Knowledge Management, CIKM ’16*, pages 929–938, New York, NY, USA, October 2016. Association for Computing Machinery. ISBN 978-1-4503-4073-1. doi: 10.1145/2983323.2983729. 1
- [35] Sudhakar Reddy Peddinti, Subba Rao Katragadda, Brij Kishore Pandey, and Ajay Tanikonda. Utilizing Large Language Models for Advanced Service Management: Potential Applications and Operational Challenges, March 2023. 1
- [36] Chao Zhang, Xuechen Liu, Katherine Ziska, Soobin Jeon, Chi-Lin Yu, and Ying Xu. Mathemyths: Leveraging Large Language Models to Teach Mathematical Language through Child-AI Co-Creative Storytelling. In *Proceedings of the 2024 CHI Conference on Human Factors in Computing Systems, CHI ’24*, pages 1–23, New York, NY, USA, May 2024. Association for Computing Machinery. ISBN 979-8-4007-0330-0. doi: 10.1145/3613904.3642647. 1
- [37] Janice Ahn, Rishu Verma, Renze Lou, Di Liu, Rui Zhang, and Wenpeng Yin. Large Language Models for Mathematical Reasoning: Progresses and Challenges, September 2024. 1
- [38] Gengze Zhou, Yicong Hong, and Qi Wu. NavGPT: Explicit Reasoning in Vision-and-Language Navigation with Large Language Models. *Proceedings of the AAAI Conference on Artificial Intelligence*, 38(7):7641–7649, March 2024. ISSN 2374-3468. doi: 10.1609/aaai.v38i7.28597. 1
- [39] Haojie Pan, Zepeng Zhai, Hao Yuan, Yaojia Lv, Ruiji Fu, Ming Liu, Zhongyuan Wang, and Bing Qin. KwaiAgents: Generalized Information-seeking Agent System with Large Language Models, January 2024. 1
- [40] Yutao Zhu, Huaying Yuan, Shuting Wang, Jiongnan Liu, Wenhan Liu, Chenlong Deng, Haonan Chen, Zheng Liu, Zhicheng Dou, and Ji-Rong Wen. Large Language Models for Information Retrieval: A Survey, September 2024. 1
- [41] Yancheng Wang, Ziyang Jiang, Zheng Chen, Fan Yang, Yingxue Zhou, Eunah Cho, Xing Fan, Xiaojiang Huang, Yanbin Lu, and Yingzhen Yang. RecMind: Large Language Model Powered Agent For Recommendation, March 2024. 1
- [42] Fang Zeng, Zhiliang Lyu, Quanzheng Li, and Xiang Li. Enhancing LLMs for Impression Generation in Radiology Reports through a Multi-Agent System, December 2024.
- [43] Shijie Han, Haoqiang Kang, Bo Jin, Xiao-Yang Liu, and Steve Y Yang. Xbrl agent: Leveraging large language models for financial report analysis. In *Proceedings of the 5th ACM International Conference on AI in Finance*, pages 856–864, 2024. 1
- [44] Hongyang Yang, Boyu Zhang, Neng Wang, Cheng Guo, Xiaoli Zhang, Likun Lin, Junlin Wang, Tianyu Zhou, Mao Guan, Runjia Zhang, and Christina Dan Wang. FinRobot: An Open-Source AI Agent Platform for Financial Applications using Large Language Models, May 2024. 1
- [45] Tushar Chugh, Kanishka Tyagi, Rolly Seth, and Pranesh Srinivasan. Intelligent agents driven data analytics using Large Language Models. In *2023 International Conference on Artificial Intelligence, Blockchain, Cloud Computing, and Data Analytics (ICoABCD)*, pages 152–157, November 2023. doi: 10.1109/ICoABCD59879.2023.10390973. 1
- [46] Andres M. Bran, Sam Cox, Oliver Schilter, Carlo Baldassari, Andrew D. White, and Philippe Schwaller. Augmenting large language models with chemistry tools. *Nature Machine Intelligence*, 6(5):525–535, May 2024. ISSN 2522-5839. doi: 10.1038/s42256-024-00832-8. 1
- [47] Alireza Ghafarollahi and Markus J. Buehler. ProtAgents: Protein discovery via large language model multi-agent collaborations combining physics and machine learning. *Digital Discovery*, 3(7):1389–1409, 2024. doi: 10.1039/D4DD00013G. 1
- [48] Mehrad Ansari and Seyed Mohamad Moosavi. Agent-based learning of materials datasets from the scientific literature. *Digital Discovery*, 3(12):2607–2617, 2024. doi: 10.1039/D4DD00252K.
- [49] Mayk Caldas Ramos, Christopher J. Collison, and Andrew D. White. A review of large language models and autonomous agents in chemistry. *Chemical Science*, 16(6):2514–2572, 2025. doi: 10.1039/D4SC03921A. 1

- [50] Yoshitaka Inoue, Tianci Song, and Tianfan Fu. DrugAgent: Explainable Drug Repurposing Agent with Large Language Model-based Reasoning, September 2024. 1
- [51] Yuchen Xia, Manthan Shenoy, Nasser Jazdi, and Michael Weyrich. Towards autonomous system: flexible modular production system enhanced with large language model agents. In *2023 IEEE 28th International Conference on Emerging Technologies and Factory Automation (ETFA)*, pages 1–8. IEEE, 2023. 1
- [52] Umair Ahmed, Rafia Mumtaz, Hirra Anwar, Sadaf Mumtaz, and Ali Mustafa Qamar. Water quality monitoring: From conventional to emerging technologies. *Water Supply*, 20(1): 28–45, October 2019. ISSN 1606-9749. doi: 10.2166/ws.2019.144. 2
- [53] Alisa L. Gallant. The Challenges of Remote Monitoring of Wetlands. *Remote Sensing*, 7(8):10938–10950, August 2015. ISSN 2072-4292. doi: 10.3390/rs70810938. 2
- [54] Zeyu Wang, Frank P-W Lo, Yunran Huang, Junhong Chen, James Calo, Wei Chen, and Benny Lo. Tactile perception: a biomimetic whisker-based method for clinical gastrointestinal diseases screening. *npj Robotics*, 1(1):3, 2023. 2
- [55] Zeyu Wang, Frank P-W Lo, Junhong Chen, James Calo, Benny PL Lo, Alex J Thompson, and Eric M Yeatman. An ai-driven bionic whisker system assisting for clinical gastrointestinal disease screening. In *2024 International Joint Conference on Neural Networks (IJCNN)*, pages 1–8. IEEE, 2024. 2
- [56] Ruiyang Zhang, Junhong Chen, Zeyu Wang, Ziqi Yang, Yunxiao Ren, Peilun Shi, James Calo, Kyle Lam, Sanjay Purkayastha, and Benny Lo. A step towards conditional autonomy-robotic appendectomy. *IEEE Robotics and Automation Letters*, 8(5):2429–2436, 2023. 2
- [57] Junhong Chen, Zeyu Wang, Ruiqi Zhu, Ruiyang Zhang, Weibang Bai, and Benny Lo. Path generation with reinforcement learning for surgical robot control. In *2022 IEEE-EMBS International Conference on Biomedical and Health Informatics (BHI)*, pages 1–4. IEEE, 2022. 2
- [58] Frank P-W Lo, Jianing Qiu, Zeyu Wang, Junhong Chen, Bo Xiao, Wu Yuan, Stamatia Giannarou, Gary Frost, and Benny Lo. Dietary assessment with multimodal chatgpt: a systematic analysis. *IEEE Journal of Biomedical and Health Informatics*, 2024. 2
- [59] Long Ouyang, Jeffrey Wu, Xu Jiang, Diogo Almeida, Carroll Wainwright, Pamela Mishkin, Chong Zhang, Sandhini Agarwal, Katarina Slama, Alex Ray, et al. Training language models to follow instructions with human feedback. *Advances in neural information processing systems*, 35:27730–27744, 2022. 3
- [60] Keith D Hjelmstad. *Fundamentals of Structural Mechanics*. Springer Science & Business Media, 2007. 3
- [61] George Keith Batchelor. *An Introduction to Fluid Dynamics*. Cambridge university press, 2000. 3
- [62] Satyandra K. Gupta, William C. Regli, Diganta Das, and Dana S. Nau. Automated manufacturability analysis: A survey. *Research in Engineering Design*, 9(3):168–190, September 1997. ISSN 1435-6066. doi: 10.1007/BF01596601. 3
- [63] Gabriella Bolzon and Vladimir Buljak. An effective computational tool for parametric studies and identification problems in materials mechanics. *Computational Mechanics*, 48(6):675–687, December 2011. ISSN 1432-0924. doi: 10.1007/s00466-011-0611-8. 3
- [64] Nam-Ho Kim, Bhavani V Sankar, and Ashok V Kumar. *Introduction to Finite Element Analysis and Design*. John Wiley & Sons, 2018. 3
- [65] Subrahmanyam Chandrasekhar. *Hydrodynamic and Hydro-magnetic Stability*. Courier Corporation, 2013. 3
- [66] Yutaro Yamada, Yihan Bao, Andrew K. Lampinen, Jungo Kasai, and Ilker Yildirim. Evaluating Spatial Understanding of Large Language Models, April 2024. 3
- [67] SOLIDWORKS. <https://www.3ds.com/products/solidworks>, January 2023. 3
- [68] Autodesk Fusion | 3D CAD, CAM, CAE, & PCB Cloud-Based Software | Autodesk. <https://www.autodesk.com/caen/products/fusion-360/overview>. 3
- [69] COMSOL: Multiphysics Software for Optimizing Designs. <https://www.comsol.com/>. 3
- [70] Earl H. Dowell and Kenneth C. Hall. MODELING OF FLUID-STRUCTURE INTERACTION. *Annual Review of Fluid Mechanics*, 33(Volume 33, 2001):445–490, January 2001. ISSN 0066-4189, 1545-4479. doi: 10.1146/annurev.fluid.33.1.445. 4
- [71] Giancarlo Alfonsi. Reynolds-Averaged Navier–Stokes Equations for Turbulence Modeling. *Applied Mechanics Reviews*, 62(040802), June 2009. ISSN 0003-6900. doi: 10.1115/1.3124648. 4
- [72] Florian R. Menter. Review of the shear-stress transport turbulence model experience from an industrial perspective. *International Journal of Computational Fluid Dynamics*, January 2009. doi: 10.1080/10618560902773387. 4
- [73] MM Rahman, V Vuorinen, J Taghinia, and M Larimi. Wall-distance-free formulation for sst $k-\omega$ model. *European Journal of Mechanics-B/Fluids*, 75:71–82, 2019. 4
- [74] A. Parente, C. Gorié, J. van Beeck, and C. Benocci. Improved $k-\varepsilon$ model and wall function formulation for the RANS simulation of ABL flows. *Journal of Wind Engineering and Industrial Aerodynamics*, 99(4):267–278, April 2011. ISSN 0167-6105. doi: 10.1016/j.jweia.2010.12.017. 4
- [75] Tan Yan and Martin D. F. Wong. Recent research development in PCB layout. In *2010 IEEE/ACM International Conference on Computer-Aided Design (ICCAD)*, pages 398–403, November 2010. doi: 10.1109/ICCAD.2010.5654190. 4
- [76] Zoltán Tafferner and Attila Géczy. Comparing large language model artificial intelligence tools in aid of electrical engineering. In *2024 IEEE 30th International Symposium for Design and Technology in Electronic Packaging (SIITME)*, pages 9–14, October 2024. doi: 10.1109/SIITME63973.2024.10814860. 4
- [77] Steve Heath. *Embedded Systems Design*. Elsevier, 2002. 5